# Formation of bound states and control of their localization in a double quantum dot at the edge of the two-dimensional topological insulator with magnetic barriers

© E.A. Lavrukhina, D.V. Khomitsky, A.V. Telezhnikov

National Research Nizhny Novgorod State University,
603950 Nizhny Novgorod, Russia

E-mail: ekaterina.a.lavrukhina@gmail.com

*Received May 6, 2023*
*Revised June 11, 2023*
*Accepted October 30, 2023*

The model of the bound states in a double quantum dot formed by three magnetic barriers at the edge of two-dimensional topological insulator based on HgTe/CdTe quantum well is developed. The peculiarities of the energy spectrum, the probability density and the spin density of the quantum states are studied as a function of the orientation of the magnetization vector for the magnetic barriers. The wavefunction localization at the left and at the right of the anticrossing point in the spectrum is studied and the conclusion is made on the possibility of switching between the states with the localization area in different quantum dots by varying the polarization of the middle barrier.

**Keywords:** topological insulator, magnetic barrier, double quantum dot, localization.

DOI: 10.61011/SC.2023.07.57419.4943C

## 1. Introduction

Topological insulators (TIs) constitute a special class of materials characterized by the presence of a band gap for bulk states and well conducting edge states topologically protected from scattering on non-magnetic impurities by time reversal symmetry [1–3]. The study of topologically protected one-dimensional states in the case of two-dimensional TI or surface states for three-dimensional TI is of great interest related to the search for methods of controlling such states and their localization, including the implementation of information storage and processing schemes on their basis. It is known that it is impossible to localize such states using purely electrostatic barriers due to Klein tunneling of massless fermions [4], so magnetic barriers can be used to create bound states [5–7], which partially destroy the scattering protection of edge states.

Over the last five years, a significant number of works have been published on the interaction of helicoidal boundary states in TI with various barriers and defects, including magnetic moments of different origin and localization. Thus, the effects of nuclear spins on the transport properties of the edge states [8], the effect of the magnetic manganese ion on the quantum dot states in HgTe-based TI [9], and the modelling of Majorana fermions in a superconductor based on the model of magnetic barriers at the edge of TI [10] were considered. A number of investigations has been performed on the phases with high Chern numbers in structures with TI and magnetic layers [11], as well as the influence of point [12] and random defect distributions on the dispersion of edge states in TI [13].

The mentioned works, which constitute only a small fraction of the published ones, testify to a rather high relevance of the topic related to the interaction of boundary states in TI with magnetic barriers and the analysis of localized states arising here. In spite of the rather wide coverage of the problems, so far, in our opinion, no unified views on the properties and potential application of localized states in quantum dot systems created on the basis of TI with the help of magnetic barriers have been developed, which determines our interest to this problem, in particular to the model of a double quantum dot created by three magnetic barriers.

For a number of years, we have been developing a model of localized states in quantum dots (QDs) formed at the edge of a two-dimensional TI based on an HgTe/CdTe quantum well using macroscopic magnetic barriers of finite permeability. In particular, on the basis of the well-known model of the interaction of an edge state with a single magnetic impurity [14], our model has recently been microscopically justified for the case of the interaction of edge states in TI with a macroscopic magnetic domain (barrier) located near the edge of TI [15]. The possibility of forming a finite number of energy levels in a one-dimensional QD, including a single pair of levels, was shown.

In this work we continue the study of bound states, but already in a double QD formed by three magnetic barriers at the edge of a two-dimensional TI based on the HgTe/CdTe quantum well. The main motivation for investigating such a system is the possibility of switching between states with wave function localization in the left and right QDs by changing only the magnetization polarization of one (central) barrier. In the mode of

antiparallel orientation of the magnetization vectors of the left and right barriers, anti-crossing points were found when the distance between the levels is minimal and the wave functions are localized with equal probability in the left and right QDs. Outside the anti-crossing band, alternating localization in the right and left QDs is observed when the orientation of the central barrier magnetization changes. Such controlled switching between states clearly delimited in space allows us to hopefully utilize the system under investigation for information storage and processing.

## 2. Model

We consider a model of quantum states in a double QD formed by magnetic barriers at the edge of a two-dimensional TI based on an HgTe/CdTe quantum well.

The double QD is formed by two outermost very wide magnetic barriers with heights (in energy units) $M_1$ and $M_2$, and a central barrier of height $M_b$ and width $L_b$. In result, a left QD with width $L_1$ and a right QD with width $L_2$ are formed. The states in the double QD can be described by the Hamiltonian, which is a generalization of the Hamiltonian from the work [15] for the case of three magnetic barriers considered in this work:

$$\begin{aligned} H = {} & Ak_y\sigma_z - M_1 S(-L_1 - y)(\sigma_x \cos\theta_1 + \sigma_y \sin\theta_1) \\ & - M_b\big(S(y) - S(y - L_b)\big)(\sigma_x \cos\theta_b + \sigma_y \sin\theta_b) \\ & - M_2 S(y - L_2 - L_b)(\sigma_x \cos\theta_2 + \sigma_y \sin\theta_2). \end{aligned} \tag{1}$$

The first summand in (1) corresponds to the effective Hamiltonian for one-dimensional helicoidal edge states with a constant $A = 360\,\text{meV}\cdot\text{nm}$ associated with the propagation velocity of states along the HgTe/CdTe [1–3] based TI edge. The remaining terms describe the effect on the boundary states from magnetic barriers, the profile of each of which is approximated by a step function $S(y)$. Such barriers can be made of magnetic dielectric materials (magnetic insulators) that do not create spin injection and do not lead to hybridization of the states of the magnet and TI. Examples include MnSe or EuS compounds, which application in TI structures has been discussed, for example, in [16,17]. The linear parameters $L_1$, $L_b$, $L_2$ specify the barrier boundaries and width of each QD. The angular parameters $\theta_1$, $\theta_b$, $\theta_2$ determine the orientations of the magnetization vectors in the plane $(x, y)$ for each of the barriers, and the energy parameters $M_1$, $M_b$, $M_2$ represent the amplitudes of the exchange interaction of the edge states with the magnetic moments of the barriers [15]. For the Hamiltonian (1) the eigenfunctions have the form of two-component spinors defined in each area of space by the expressions

$$\begin{cases} \psi_{y<-L_1} = B \begin{pmatrix} 1 \\ -\frac{i\sqrt{M_1^2 - E^2} + E}{M_1} e^{i\theta_1} \end{pmatrix} e^{\frac{\sqrt{M_1^2 - E^2}}{A} y}, \\ \psi_{QD1} = \begin{pmatrix} C_1 e^{\frac{iEy}{A}} \\ C_2 e^{-\frac{iEy}{A}} \end{pmatrix}, \\ \psi_{0<y<L_b} = D_1 \begin{pmatrix} 1 \\ \frac{i\sqrt{M_b^2 - E^2} - E}{M_b} e^{i\theta_b} \end{pmatrix} e^{-\frac{\sqrt{M_b^2 - E^2}}{A} y} \\ + D_2 \begin{pmatrix} 1 \\ -\frac{i\sqrt{M_b^2 - E^2} + E}{M_b} e^{i\theta_b} \end{pmatrix} e^{\frac{\sqrt{M_b^2 - E^2}}{A} y}, \\ \psi_{QD2} = \begin{pmatrix} H_1 e^{\frac{iEy}{A}} \\ H_2 e^{-\frac{iEy}{A}} \end{pmatrix}, \\ \psi_{y>L_b+L_2} = J \begin{pmatrix} 1 \\ \frac{i\sqrt{M_2^2 - E^2} - E}{M_2} e^{i\theta_2} \end{pmatrix} e^{-\frac{\sqrt{M_2^2 - E^2}}{A} y}. \end{cases} \tag{2}$$

Taking advantage of the continuity conditions of the wave function at the boundaries of the barriers $y = -L_1$, $y = 0$, $y = L_b$ and $y = L_b + L_2$, we obtain a system of linear equations with respect to the coefficients $B$, $C_{1,2}$, $D_{1,2}$, $H_{1,2}$, $J$. The existence of a nontrivial solution of the system (2) takes place under the condition that its determinant is zero, which leads to the characteristic equation for the energy $E$ of discrete levels in the double QD. Next, we describe the solutions of the system (2) for such values of the parameters at which it is possible to control the localization band of the wave functions.

## 3. Dependence of wave function localization on polarization of barriers

After finding the coefficients for the wave function (2), its localization band can be described through the sum of the coefficients $|C_1|^2 + |C_2|^2$ for the left QD and through the sum of $|H_1|^2 + |H_2|^2$ for the right QD. Let us introduce the ratio of these probabilities

$$P \equiv \frac{|C_1|^2 + |C_2|^2}{|H_1|^2 + |H_2|^2}, \tag{3}$$

which will characterize the localization of the corresponding wave function: at $P \gg 1$ the wave function is localized in the left QD, and at $P \ll 1$ — in the right QD. The question arises — how does the relation (3) for a given energy level change when the system parameters are changed. Consider the mode of antiparallel orientation of the magnetization of the left and right barriers $\theta_1 = 0$, $\theta_2 = \pi$. Figure 1 shows the structure of the system levels depending on the orientation of the magnetization of the central barrier $\theta_b$. Other system parameters $L_{1,2,b} = 100\,\text{nm}$, $M_{1,2,b} = 20\,\text{meV}$. On each

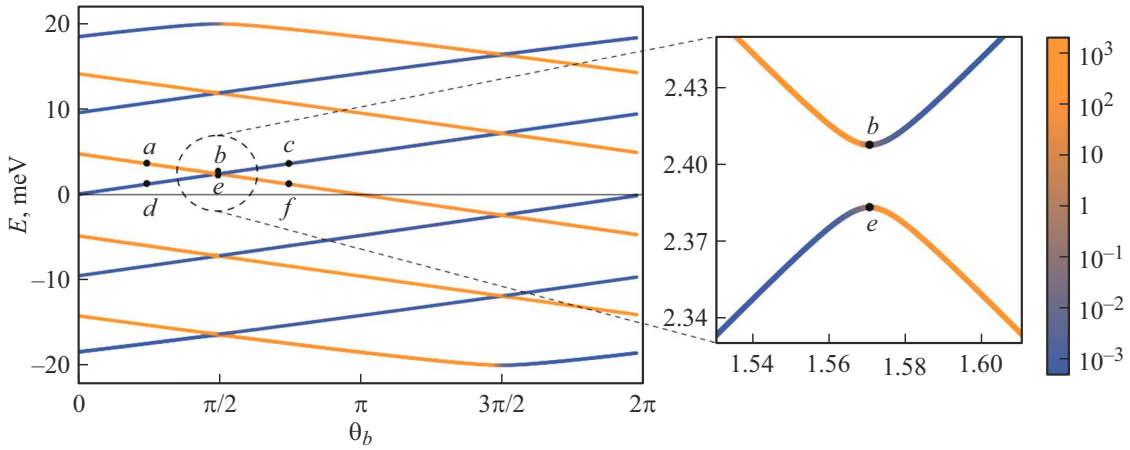


**Figure 1.** Energy spectrum as a function of the magnetization angle of the central barrier at $\theta_b$ at $\theta_1 = 0$, $\theta_2 = \pi$, $L_{1,2,b} = 100$ nm, $M_{1,2,b} = 20$ meV. Blue shows states with localization in the right QD when the ratio (4) $P \ll 1$, orange — states with localization in the left QD at $P \gg 1$. The inset on the right shows the anti-crossing band for the dashed highlighted band when the wave functions of levels $(b, e)$ are localized simultaneously in two QDs. (The colored version of the figure is available on-line).

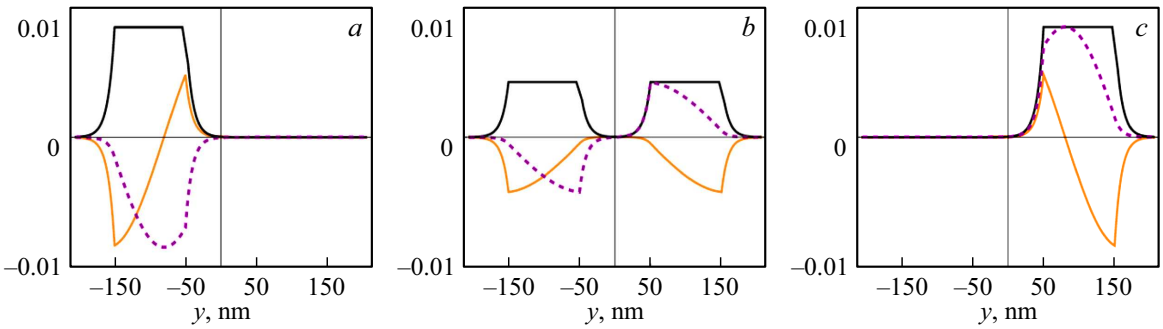


**Figure 2.** Distributions along the double quantum dot structure for the probability density $|\psi|^2$ (black solid line) and spin densities $S_x$ (lilac dashed line), $S_y$ (orange solid line) for the energy levels $(a, b, c)$ marked in Figure 1. (The colored version of the figure is available on-line).

line, the relationship (3) is shown in color. In the -orange and yellow bands, the wave function is almost completely localized in the left QD, and in the blue and cyan bands — in the right QD. For points on the spectrum $(a-c)$, the probability and spin densities are shown further in Figure 2. The inset on the right in Figure 1 shows the band of level convergence (anti-crossing) for the dotted band on the left, when the wave functions of levels $(b, e)$ are localized simultaneously in two quantum dots. From Figure 1 we can conclude that the spectrum contains anti-crossing at the orientation of the central barrier magnetization $\theta_b = \frac{\pi}{2}$ and $\theta_b = \frac{3\pi}{2}$,while the convergence of levels is determined by the permeability of the central barrier. By expanding the dispersion equation near the anti-crossing point, we can obtain an estimate for the magnitude of the slit in Figure 1 in the form $\Delta \sim (AM/L)^{1/2} \exp(-LM/A)$. For the parameters in Figure 1 we obtain that $\Delta = 0.033$ meV, which is a good approximation for the results of the numerical calculation presented in Figure 1. Note that the slit $\Delta$ has a maximum at a small barrier height $M_0 = A/2L = 1.8$ meV, equal to $\Delta_m \sim 1.5$ meV, and then decreases with increasing $M$. However, for applications in building qubits, such low barriers and wide gaps in the spectrum are of little use. The anti-crossing point is the point of change of the localization band of the wave function for this level, as can be seen from Figure 1. This effect appears to be robust to small variations in the system parameters, since the levels of one doublet away from the anti-crossing points are separated by a significant gap from the other doublets, as can be seen in Figure 1.

The localization of the wave function for specific states can be clearly shown by visualizing the probability density and spin projection densities. Figure 2 shows in relative units the probability density $|\psi|^2$ and spin densities $S_{x,y} = \psi^+ \sigma_{x,y} \psi$ for points $(a, b, c)$ in the spectrum in Figure 1. The absolute probability of finding an electron in the left or right QD can be obtained by integrating $|\psi|^2$ over the given QD and is a value close to unity for Figure 2, $a, c$ and to 1/2 at each point for Figure 2, $b$ if the contribution from the barrier band is neglected. The third projection of spin $S_z$ for states (2) in our model is identically zero [15]. It can be seen that as the angle $\theta_b$ passes through the anti-crossing point, the localization area of the wave function changes from $(a)$ localization in the left QD, $(b)$

localization in both QDs at the anti-crossing point, and ($c$) localization in the right QD. A similar process is observed for the levels ($d$–$f$) in Figure 1 with the reverse sequence of localization areas. As can be seen from Figure 1, the change interval $\theta_b$ near the anti-crossing point for the localization band change can be relatively small, $\sim 20-30^\circ$, which should facilitate this state localization control mechanism.

## 4. Conclusion

A model of bound states in a double quantum dot at the edge of a topological insulator based on an HgTe/CdTe quantum well formed by three magnetic barriers is constructed. The features of the energy spectrum, probability density and spin density depending on the parameters of magnetic barriers are considered. Anti-crossing points were found to depend on the polarization of the central barrier, to the left and right of which localization of wave functions in different quantum dots is observed. The considered methods of controlling the localization of wave functions at the edge of the topological insulator indicate the promising use of such structures for the creation of new qubit circuits.

### Acknowledgments

The authors are grateful to A.A. Konakov, V.Ya. Aleshkin and I.S. Burmistrov for numerous useful discussions.

### Funding

The work was supported by the Ministry of Science and Higher Education of the RF under State Assignment FSWR-2023-0035.

### Conflict of interest

The authors declare that they have no conflict of interest.

## References

[1] B.A. Bernevig. *Topological Insulators and Topological Superconductors* (Princeton University Press, Princeton, 2013) p. 117.
[2] X.-L. Qi, S.-C. Zhang. Rev. Mod. Phys., **83**, 1057 (2011). DOI: 10.1103/RevModPhys.83.1057
[3] B.A. Bernevig, T.L. Hughes, S.-C. Zhang. Science, **314**, 1757 (2006). DOI: 10.1126/science.1133734
[4] M.I. Katsnelson, K.S. Novoselov, A.K. Geim. Nature Physics, **2**, 620 (2006). DOI: 10.1038/nphys384
[5] C. Timm. Phys. Rev. B, **86**, 155456 (2012). DOI: 10.1103/PhysRevB.86.155456
[6] G. Dolcetto, N. Traverso Ziani, M. Biggio, F. Cavaliere, M. Sassetti. Phys. Rev. B, **87**, 235423 (2013). DOI: 10.1103/PhysRevB.87.235423
[7] G.J. Ferreira, D. Loss. Phys. Rev. Lett., **111**, 106802 (2013). DOI: 10.1103/PhysRevLett.111.106802
[8] C.-H. Hsu, P. Stano, J. Klinovaja, D. Loss. Phys. Rev. B, **97**, 125432 (2018). DOI: 10.1103/PhysRevB.97.125432
[9] X. Li, Z. Wu, W. Lou. Sci. Rep., **9**, 9080 (2019). DOI: 10.1038/s41598-019-45067-5
[10] N. Travserso Ziani, C. Fleckenstein, L. Vigliotti, B. Trauzettel, M. Sassetti. Phys. Rev. B. **101**, 195303 (2020). DOI: 10.1103/PhysRevB.101.195303
[11] Y.-X. Wang, F. Li. Phys. Rev. B, **104**, 035202 (2021). DOI: 10.1103/PhysRevB.104.035202
[12] V.A. Sablikov. A.A. Sukhanov. Phys. Rev. B, **103**, 155424 (2021). DOI: 10.1103/PhysRevB.103.155424
[13] S. Wolski, M. Inglot, C. Jasiukiewicz, K.A. Kouzakov, T. Masłowski, T. Szczepa.ski, S. Stagraczyński, R. Stagraczyński, V.K. Dugaev, L. Chotorlishvili. Phys. Rev. B, **106**, 224418 (2022). DOI: 10.1103/PhysRevB.106.224418
[14] P.D. Kurilovich, V.D. Kurilovich, I.S. Burmistrov, M. Goldstein. Phys. Rev. B, **94**, 155408 (2016). DOI: 10.1103/PhysRevB.94.155408
[15] D.V. Khomitsky, A.A. Konakov, E.A. Lavrukhina. J. Phys.: Condens. Matter, **34**, 405302 (2022). DOI: 10.1088/1361-648X/ac8407
[16] W. Luo, X.-L. Qi. Phys. Rev. B, **87**, 085431 (2013). DOI: 10.1103/PhysRevB.87.085431
[17] A.G. Mal'shukov. Phys. Rev. B, **90**, 045311 (2014). DOI: 10.1103/PhysRevB.90.045311

*Translated by Ego Translating*